J Therm Anal Calorim
DOI 10.1007/s10973-016-5445-3

Thermal behavior of new nickel(II) complexes with unsaturated carboxylates and heterocyclic N-donor ligands

Rodica Olar[1] · Ioana Dorina Vlaicu[1,2] · Mariana Carmen Chifiriuc[3] · Coralia Bleotu[4] · Nicolae Stănică[5] · Gina Vasile Scăeţeanu[6] · Luigi Silvestro[7] · Constanţa Dulea[8] · Mihaela Badea[1]

Received: 30 October 2015 / Accepted: 3 April 2016

Abstract Synthesis and characterization of four new Ni(II) complexes with mixed ligands have been reported in the present paper. As interest ligands, acrylate (acr) ion together with one N-donor heterocyclic ligand, namely benzimidazole (HBzIm), 2-methylbenzimidazole (2-MeBzIm), 5-methylbenzimidazole (5-MeBzIm) or 5,6-dimethylbenzimidazole (5,6-Me_2BzIm), was chosen. The syntheses afforded the complexes formulated as $[Ni(HBzIm)_2(acr)_2(H_2O)]\cdot 3H_2O$ (**1**), $[Ni(2\text{-}MeBzIm)_2(acr)_2(H_2O)]\cdot 1.5H_2O$ (**2**), $[Ni(5\text{-}MeBzIm)_2(acr)_2(H_2O)]$ (**3**) and $[Ni(5,6\text{-}Me_2BzIm)_2(acr)_2]$ (**4**). Complexes (**1**) and (**2**) contain crystallization water molecules and coordinated water molecules, both their nature and presence being confirmed on the basis of IR spectra and thermal analysis. In contrast to above-mentioned complexes, (**3**) contains only coordinated water molecule, while (**4**) is an anhydrous compound. Based on electronic spectra and magnetic measurements, a distorted octahedral stereochemistry was proposed for all Ni(II) complexes. Acrylate ions act both as unidentate and chelate ligands in complexes (**1**)–(**3**), while in complex (**4**) act only as chelate ligands. All used N-donor ligands function as monodentate in all Ni(II) complexes. Biological properties of complexes (**1**)–(**4**) were evaluated against several Gram(+), Gram(−) bacterial strains and against fungus *Candida albicans*.

Keywords Nickel complexes · Thermal analysis · Acrylate · Benzimidazole · Antimicrobial activity

Introduction

The presence of benzimidazole and its derivatives in coordination chemistry has gained a lot of importance and received considerable attention because of their biological significance and interesting structural aspects [1].

Benzimidazole derivatives represent an important class of bioactive molecules that play an important role in medical area. The benzimidazole core is found in the structure of some drugs (albendazole, fenbendazole, thiabendazole, inhibitors of proton pump) used in both human and veterinary medicine [2]. Moreover, their metal complexes exhibit anticancer [3, 4], antibacterial [5], SOD activities [6], fluorescent [7] and magnetic [4] properties.

Electronic supplementary material The online version of this article (doi:10.1007/s10973-016-5445-3) contains supplementary material, which is available to authorized users.

✉ Mihaela Badea
e_m_badea@yahoo.com

[1] Department of Inorganic Chemistry, Faculty of Chemistry, University of Bucharest, 90-92 Panduri Str., 050663 Bucharest, Romania

[2] National Institute of Materials Physics, Atomistilor Str. 405A, POB MG-7, Măgurele, 077125 Ilfov, Romania

[3] Department of Microbiology, Faculty of Biology, University of Bucharest, 1-3 Aleea Portocalelor Str., 60101 Bucharest, Romania

[4] Stefan S Nicolau Institute of Virology, 285 Mihai Bravu Ave., Bucharest, Romania

[5] Romanian Academy, "Ilie Murgulescu" Physical Chemistry Institute, 202 Splaiul Independentei, 77208 Bucharest, Romania

[6] Department of Soil Sciences, University of Agronomical Sciences and Veterinary Medicine, 59 Mărăşti Str., Sector 1, 011464 Bucharest, Romania

[7] 3S-Pharmacological Consultation and Research GmbH, 1 Koenigsbergerstrasse, 27243 Harpstedt, Germany

[8] Pharma Serv. International SRL, 52 Sabinelor Str., Sector 5, 050853 Bucharest, Romania

Published online: 13 April 2016

Besides above-mentioned properties, benzimidazole-based complexes present higher catalytic effect on the degradation of Congo red in the Fenton-like system [8] or efficiently catalyze the controllable polymerization of methyl methacrylate [9].

The literature data revealed that both type and substituent position (1-, 2- or 5-) on benzimidazole ring are responsible for their wide range of pharmaceutical properties and the inclusion of benzimidazole moiety in various complexes represents an efficient strategy for designing biologically active compounds [4, 10, 11].

Benzimidazole "6 + 5" heterocyclic structure is encountered also in the case of purines and from this structural similarity arises the biological activities of benzimidazole and its derivatives. For instance, it is possible that these antibacterial properties of benzimidazoles to be attributed to their competition with purines, thus leading to the inhibition of the synthesis of bacterial nucleic acids and proteins [12].

Furthermore, in the nature appears the most important benzimidazole derivative, namely N-ribosyl-dimethylbenzimidazole, which acts as axial ligand for cobalt in B_{12} vitamin [13].

In the literature are reported two categories of complexes that possess benzimidazole moiety and carboxylate groups: (**i**) mixed ligand complexes based on benzimidazole/benzimidazole derivative and various carboxylic acids [6, 7, 14–16] and (**ii**) complexes with ligands that contain benzimidazole core with grafted carboxylate groups [17–20], both categories presenting interesting architectures and properties.

In our ongoing efforts to synthesize and characterize mixed complexes with N-donor ligands and carboxylic acids [21–24], we report herein the results related to synthesis, physicochemical characterization and biological activity of four new nickel(II) complexes with acrylate (acr) ion and benzimidazole (HBzIm) or benzimidazole derivatives (2-methylbenzimidazole (2-MeBzIm)/5-methylbenzimidazole (5-MeBzIm)/5,6-dimethylbenzimidazole (5,6-Me_2BzIm)) as ligands.

Experimental

For synthesis of complexes, all reagents were purchased and used as received from Sigma-Aldrich, Germany. The raw materials involved in nickel acrylate synthesis are nickel carbonate basic hydrate ($NiCO_3.Ni(OH)_2{\cdot}xH_2O$, 99.9 %) and anhydrous prop-2-enoic acid (acrylic acid) ($C_3H_4O_2$, 99 %). As ligands are also used benzimidazole ($C_7H_6N_2$, 98 %), 2-methylbenzimidazole ($C_8H_8N_2$, 98 %), 5-methylbenzimidazole ($C_8H_8N_2$, 98 %) and 5,6-dimethylbenzimidazole ($C_9H_{10}N_2$, ≥99 %) (Scheme 1).

Synthesis of Ni(II) complexes with acrylate and benzimidazole/benzimidazole derivatives

A simple procedure was approached in order to obtain new complexes [23, 24]: Nickel(II) acrylate was freshly prepared by direct reaction between nickel(II) carbonate hydrate (4 g, 13 mmol) (molar ratio 1:6) and anhydrous acrylic acid (5.43 mL, 80 mmol) in methanol (250 mL) at 100 °C. Then, the freshly prepared nickel(II) acrylate (1 g, 3.66 mmol) was mixed with benzimidazolic ligand (L = benzimidazole (HBzIm, 0.866 g, 7.33 mmol), 2-methylbenzimidazole (2-MeBzIm, 0.969 g, 7.33 mmol), 5-methylbenzimidazole (5-MeBzIm, 0.969 g, 7.33 mmol) and 5,6-dimethylbenzimidazole (5,6-Me_2BzIm, 1.072 g, 7.33 mmol)) in 1:2 molar ratio. This method afforded four blue nickel(II) complexes labeled (**1**)–(**4**) further in the manuscript, which present weak solubility in methanol, dimethylsulfoxide and N,N-dimethylformamide.

The new synthesized compounds (**1**)–(**4**) are blue colored, stable in air and light at room temperature. Results of elemental analyses are in good agreement with the calculated values of elements abundances in the proposed compounds, as follows:

[Ni(HBzIm)$_2$(acr)$_2$(H$_2$O)]·3H$_2$O (**1**) Analysis, found: Ni, 11.38; C, 47.30; H, 5.03; N, 10.85 %; calculated for $NiC_{20}H_{26}N_4O_8$ (F.W. = 509.13): Ni, 11.53; C, 47.18; H, 5.15; N, 11.00 %.

[Ni(2-MeBzIm)$_2$(acr)$_2$(H$_2$O)]·1.5H$_2$O (**2**) Analysis, found: Ni, 11.38; C, 51.50; H, 5.30; N, 11.13 %; calculated for $NiC_{22}H_{27}N_4O_{6.5}$ (F.W. = 510.16): Ni, 11.50; C, 51.79; H, 5.33; N, 10.98 %.

[Ni(5-MeBzIm)$_2$(acr)$_2$(H$_2$O)] (**3**) Analysis, found: Ni, 12.08; C, 54.30; H, 5.20; N, 11.43 %; calculated for $NiC_{22}H_{24}N_4O_5$ (F.W. = 483.14): Ni, 12.15; C, 54.69; H, 5.00; N, 11.60 %.

[Ni(5,6-Me$_2$BzIm)$_2$(acr)$_2$] (**4**) Analysis, found: Ni, 12.08; C, 58.30; H, 5.30; N, 11.23 %; calculated for $NiC_{24}H_{26}N_4O_4$ (F.W. = 493.18): Ni, 11.90; C, 58.45; H, 5.31; N, 11.36 %.

Materials and methods

Chemical analysis has been performed using a EuroEA elemental analyzer (for C, N and H) and a Shimadzu AA 6300 spectrometer (for metallic ion).

Infrared spectra were recorded on KBr pellets with a Bruker Tensor 37 spectrometer in the range 400–4000 cm^{-1}.

Electronic spectra by diffuse reflectance technique, with Spectralon as standard, were recorded in the range 200–1500 nm, on a Jasco V670 spectrophotometer.

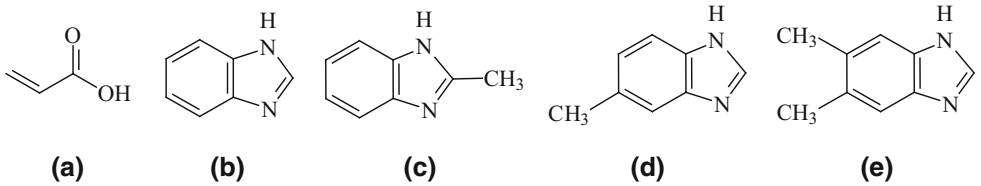

Scheme 1 Structural formula of **a** acrylic acid, **b** benzimidazole (HBzIm), **c** 2-methylbenzimidazole (2-MeBzIm), **d** 5-methylbenzimidazole (5-MeBzIm), **e** 5,6-diemthylbenzimidazole (5,6-Me_2BzIm)

Magnetic measurements were effectuated at room temperature, on a Lake Shore's fully integrated vibrating sample magnetometer (VSM) system 7404 and calibrated with a Ni sphere. The molar magnetic susceptibilities were calculated and corrected for the atomic diamagnetism.

Mass spectra were recorded with API 5000 ABSCIEX-Canada mass spectrometer with ESI source (Turbo spray model ABSCIEX) operating in positive mode. Samples were dissolved in methanol at 10 μg mL^{-1}. Molecular ions scanning range (*m/z*) was 0–1250.

The X-ray powder diffraction patterns were collected on a DRON-3 diffractometer with a nickel filtered Cu K_α radiation ($\lambda = 1.5418$ Å) in 2θ range of 10°–115°, a step width of 0.02° and an acquisition time of 0.5 s per step.

For *thermal analysis* the heating curves (TG and DTA) were recorded using a Labsys 1200 SETARAM instrument, with a sample mass of 6–12 mg over the temperature range of 30–900 °C, using a heating rate of 10 K min^{-1}. The measurements were carried out in synthetic air (flow rate 16.66 cm^3 min^{-1}) using alumina crucibles.

The antimicrobial activities of the complexes were determined against ATCC reference and clinical microbial strains, i.e., Gram-positive (*Staphylococcus aureus* ATCC 6538, *Bacillus subtilis* ATCC 6683, *Enterococcus faecium* E5), Gram-negative (*Klebsiella pneumoniae* IC 13420, *Escherichia coli* ATCC 25922, *Pseudomonas aeruginosa* ATCC 27857) and fungus *Candida albicans* 1760.

Microbial suspensions [1.5×10^8 CFU mL^{-1}; colony-forming units (CFU)] corresponding to 0.5 McFarland density obtained from 15 to 18 h bacterial cultures developed on solid media were used. The antimicrobial activity was tested on Mueller–Hinton agar medium, while a medium of yeast peptone glucose was used in case of *C. albicans*. The compounds were solubilized in DMSO, and the starting stock solution was of 1000 μg mL^{-1} concentration.

Quantitative assay of the antimicrobial activity was carried out by liquid medium microdilution method, in 96-multiwell plates, in order to determine the minimal inhibitory concentration (MIC/μg mL^{-1}). In this purpose, serial twofold dilutions of the compounds ranging between 1000 and 1.95 μg mL^{-1} were performed in 200 μL volume of broth and each well was seeded with 50 μL microbial inoculums. Sterility control (wells containing only culture medium) and culture controls (wells containing culture medium seeded with the microbial inoculums) were used. The influence of the DMSO solvent was quantified also in a series of wells containing DMSO that was diluted accordingly with the dilution scheme used for the complexes. The plates incubated for 24 h at 37 °C, and MIC values considered as the lowest concentration of the tested compound that inhibited the visible growth of the microbial overnight cultures.

The assessment of the complexes influence on the microbial ability to colonize an inert substratum has been carried out by the microtiter method. The absorbance read at 490 nm with an ELISA reader Apollo LB 911. All biological experiments performed in triplicates.

Cytotoxicity assay

Cell cycle assay was studied on HCT-8 cell line (ATCC® CCL-244™). This was cultivated in RPMI 1640 (Gibco, NY, SUA) supplemented with 10 % heat-inactivated bovine serum and penicillin/streptomycin at 37 °C with 5 % CO_2. The adherent cells were detached, centrifuged, suspended in fresh medium, counted by trypan blue exclusion and adjusted to 5×10^4 cells mL^{-1} and then were cultivated in 6-well plate and treated for 24 h with 100 μg mL^{-1} compound. After treatment period, cells were taken from the substrate, fixed in 70 % cold ethanol for at least 30 min at −20 °C, washed twice in phosphate-buffered saline (PBS) and then incubated 15 min at 37 °C with RNAse A (100 μg mL^{-1}) and 1 h with propidium iodide (100 μg mL^{-1}). After staining of cells with propidium iodide, the acquisition was done using Epics Beckman Coulter flow cytometer. Data were analyzed using FlowJo software and expressed as fractions of cells in the different cell cycle phases [25].

Results and discussion

Previously reported studies [23, 24] evidenced that complexes with carboxylate and azole-type ligands present a great interest, their chemistry correlated with their biological potential making them future candidates for more

detailed studies. This is due to the fact that imidazole nucleus is the "heart" of a large number of natural and pharmacologically active products [26]. In light of the above mentioned, herein are presented the synthesis and characterization of four new nickel(II) complexes which bear acrylate and azole ligands (benzimidazole (HBzIm)/2-methylbenzimidazole (2-MeBzIm)/5-methylbenzimidazole (5-MeBzIm)/5,6-dimethylbenzimidazole (5,6-Me_2BzIm).

These new compounds were formulated using experimental techniques like elemental analysis, NIR-UV–Vis, mass and infrared spectroscopies, magnetic moments measurements and thermal analysis. Moreover, there was performed an evaluation for a possible use as pharmacological agents, by antimicrobial assays and cytotoxicity effects investigations.

Taking into account that thermal analysis is a useful and accessible method for achievement of molecular compositions [23, 24], thermal analysis was employed in this paper to find quantitative information about our new nickel complexes.

Infrared spectroscopy

The characteristic infrared bands for nickel complexes (**1**)–(**4**) and their assignments, according to the literature data regarding analogous Ni(II) complexes [27–32], are presented in Table 1. Infrared spectra (see supplementary material, Fig. 1S) confirmed the presence in complexes of some functional individual groups.

Thus, the bands characteristic to stretching vibration of secondary amine group, ν(N–H), together with that of methine group, ν(C–H), indicates the presence of benzimidazole derivatives in their neutral form [33]. Furthermore, the bands associated with the imidazolic ν(C=N) group in the free ligands (1587, 1585, 1587 and 1590 cm^{-1}) are slightly shifted toward lower energies in the spectra of complexes (**1**)–(**4**) (1595, 1593, 1592 and 1594 cm^{-1}), indicating that the benzimidazoles are bound to the metals through the nitrogen atom [27, 31]. The negative shift of ν(C=N) stretch in the complexes indicates involvement of the azomethine nitrogen in complexation [28]. The strong band from 1245 cm^{-1} assigned to the benzimidazole ring is shifted to higher energies in all complexes spectra; this aspect together with the decrease of its intensity indicates that benzimidazole ligands are coordinated to metal by pyridine-type nitrogen atom in these complexes [28].

Acrylate coordination mode was assigned based on the presence of two characteristic modes associated with antisymmetric ν_{as}(COO) and symmetric ν_s(COO) stretching vibration modes for carboxylate group. According to literature data [34–37], the difference between these two carboxylate characteristic bands is defined by Δ criterion. The values calculated for Δ criterion in the case of these new nickel complexes (**1**)–(**4**), and based on the values the coordination modes assigned to acrylate ligands, are presenting below, in Table 2:

Both unidentate and chelate bidentate coordination modes were highlighted in complexes (**1**), (**2**) and (**3**), while for complex (**4**) the acrylato anion acts only as bidentate.

The presence of water molecules in complexes (**1**), (**2**) and (**3**) was evidenced by the presence of the stretching vibration mode ν(OH) around 3400 cm^{-1}. For complexes (**1**), (**2**) and (**3**), the presence of the band around 830 cm^{-1} assigned for the vibration mode $\rho_r(H_2O)$ indicated the presence of water molecules in the coordination sphere of nickel complexes [33].

Electronic spectroscopy

The absorption maxima, the band assignment and values of magnetic moments are summarized in Table 3. The presence in electronic spectra (see supplementary material, Fig. 2S) of the bands around 9300, 15,500 and 25,600 cm^{-1} in electronic spectra of all four Ni(II) complexes (**1**)–(**4**) suggests an octahedral distorted stereochemistry [38, 39]. The values of magnetic moments range between 2.80 and 3.50 BM, behavior specific to the nickel (II) ion found in an octahedral distorted stereochemistry with the ground term $^3A_{1g}$ [40, 41].

The values for crystal field parameters were calculated based on the absorption maxima using König's formulas [42]. The calculated 10Δq values for complexes (**1**)–(**4**) are around 9300 cm^{-1}, which are close to 9400 cm^{-1} value reported in the literature for the corresponding $[NiN_2O_4]$ chromophore [38, 43].

The presence of oxygen donor atoms (originates from acrylates) is associated with a low field which generates crystal field parameters with low values (Table 3). nephelauxetic parameter (β) values correspond to a high degree of ionic character due of the interactions with acrylate anion [42, 43], this being in agreement with our hypothesis.

In the electronic spectra of complexes (**1**)–(**4**), in the range 36,000–38,000 cm^{-1}, appear bands, which can be assigned to π–π^* transitions resulted from C=N group of benzimidazole derivatives.

The intensities and positions of absorption bands observed in NIR-UV–Vis spectra indicated that benzimidazole is *cis*-positioned in complex (**1**). Furthermore, considering the possible hindrance induced by methyl substituents in complexes (**2**), (**3**) and (**4**), the *trans* position of benzimidazole derivatives could be assumed.

Table 1 Characteristic absorption bands (cm^{-1}) in IR spectra of complexes (**1**)–(**4**)

NaAcr	HBzIm	2-MeBzIm	5-MeBzIm	5,6-diMeBzIm	(1)	(2)	(3)	(4)	Assignments
–	–	–	–	–	3440 w	3468 m	3420 w	–	ν (OH_2)
–	3113 w	3062 m	3016 w	3019 m	3110 w	3197 m	3122 w	2968 m	ν (CH)
	3061 w	2995 m		2963 m					ν (NH)
	3011 w								
	2973 w								
	2969 w								
2920 w	–	–	–	–	2906 w	2900 w	2915 w	2930 m	ν_{as} (CH_2)
2880 w	–	–	–		2880 w	2870 w	2880 w	2864 w	ν_s (CH_2)
–	2539 w	2545 w	2535 w	2535 w	–	–	–	–	δ (benzene ring)
–	1587 m	1585 w	1587 m	1590 m	1595 s	1593 s	1592 vs	1594 vs	ν (C=N)
1571 vs	–	–	–	–	1570 m	1557 vs	1575 s	1570 s	ν_{as} (COO)
1520 m	–	–	–	–	1537 m	1535 s	1530 s	1525 s	ν (C=C)
–	1495 w	1487 m	1495 w	1499 m	1492 s	–	1491 s	1490 s	γ (CH from benzene ring)
–	1477 m		1475 vs	1473 vs	1455 m	1456 m	–	–	ν (ring)
	1457 vs	1450 vs	1444 vs	1440 vs					
	1408 vs	1416 vs	1415 s	1406 s					
1368 m	–	–	–	–	1423 vs	1426 s	1424 vs	1425 vs	ν_s (COO)
					1363 s	1354 s	1362 vs		
–	1363 m	1361 m	1339 s	1335 s	1303 m	1295 w	1299 s	1315 m	ν (ring)
	1345 m								
	1300 m	1290 m							
1280 m	–	–	–	–	1270 m	1279 m	1275 m	1280 m	δ (CH_2)
–	1271 m	1271 vs	1281 vs	1268 vs	1264 m	1265 w	1254 m	1268 m	δ (benzene ring)
–	1244 s	1219 s	1248 vs	1239 vs	–	1222 w	–	–	ν (ring)
–	1201 m	1200 w	1190 m	1195 w	1198 w	–	1193 s	1197 s	δ (CH from benzene ring)
–	1132 m	1130 w	1135 m	1158 s	1154 w	1130 w	1125 w	–	δ (NH)
–	957 m	950 w	954 vs	954 vs	963 m	957 m	961 m	961 m	δ (CH from imidazole ring)
–	932 m	905 w	905 w	900 w	–	930 w	–	–	δ (benzene ring)
–	886 m	885 w	866 m	864 vs	875 w	870 w	865 m	870 m	δ (imidazole ring)
–	–	–	–	–	834 m	835 m	830 m	–	ρ_r (OH_2)
–	768 m	770 m	770 m	770 m	770 w	–	770 w	–	δ (imidazole ring)
–	745 vs	734 vs	740 m	745 w	744 s	745 vs	–	–	γ (CH from benzene ring)
–	625 m	635 w	632 s	647 m	653 m	654 m	653 s	653 m	γ (NH) + δ (imidazole ring) + τ (imidazole ring)
	617 w		603 s		617 w		622 m	613 m	
	577 w								
–	541 w	537 w	–	555 m	525 w	550 w	500 m	560 w	τ (ring)

vs* very strong, *s* strong, *m* medium, *w* weak (bands intensity in FTIR spectra), *HBzIm* benzimidazole, *2-MeBzIm* 2-methylbenzimidazole, *5-MeBzIm* 5-methylbenzimidazole, *5,6-Me_2BzIm* 5,6-dimethylbenzimidazole, (1**)—$[Ni(HBzIm)_2(acr)_2(H_2O)]\cdot 3H_2O$; (**2**)—$[Ni(2\text{-}MeBzIm)_2(acr)_2(H_2O)]\cdot 1.5H_2O$; (**3**)—$[Ni(5\text{-}MeBzIm)_2(acr)_2(H_2O)]$; (**4**)—$[Ni(5,6\text{-}Me_2BzIm)_2(acr)_2]$; ν—stretching; δ—in plane bending; γ—out of plane bending; τ—torsion

Mass spectra

The ESI–MS spectra recorded in positive ionization mode contain peaks corresponding to $[NiL_2acr_2 + H]^+$ ion at *m/z*: 438/466/466/494 for complexes (**1**)/(**2**)/(**3**)/(**4**), respectively (Fig. 1). Some other resulted fragments from complexes are evidenced: $[NiL_2acr]^+$ (*m/z*: 366/394/394/422), $[NiLacr_2 + H]^+$ (*m/z*: 320/334/334/348), $[NiLacr]^+$ (*m/z*: 248/262/262/276) as well as the protonated ligands $[L + H]^+$ (*m/z*: 119/133/133/147).

Table 2 Coordination mode assignment for acrylate anion in complexes (**1**)–(**4**)

Complex	$\Delta(COO^-)/cm^{-1}$	Coordination mode for acrylate anions
$[Ni(HBzIm)_2(acr)_2(H_2O)]\cdot 3H_2O$ (1)	147	Chelate bidentate
	207	Unidentate
$[Ni(2\text{-}MeBzIm)_2(acr)_2(H_2O)]\cdot 1.5H_2O$ (2)	131	Chelate bidentate
	203	Unidentate
$[Ni(5\text{-}MeBzIm)_2(acr)_2(H_2O)]$ (3)	151	Chelate bidentate
	213	Unidentate
$[Ni(5,6\text{-}Me_2BzIm)_2(acr)_2]$ (4)	145	Chelate bidentate

Table 3 NIR–UV–Vis absorption bands and calculated magnetic moments for complexes (**1**)–(**4**)

Complex	Absorption maximum/cm^{-1}	Assignments	Crystal field parameters			μ_{ef} (B.M.)
			$10\Delta q/cm^{-1}$	B/cm^{-1}	β	
$[Ni(HBzIm)_2(acr)_2(H_2O)]\cdot 3H_2O$ **(1)**	36,360	$\pi \rightarrow \pi^*$	9302	883	0.85	3.20
	25,640	$^3A_{1g} \rightarrow {}^3T_{1g}$ (P)				
	15,500	$^3A_{1g} \rightarrow {}^3T_{1g}$				
	13,500	$^3A_{1g} \rightarrow {}^1E_g$				
	9300	$^3A_{1g} \rightarrow {}^3T_{2g}$				
$[Ni(2\text{-}MeBzIm)_2(acr)_2(H_2O)]\cdot 1.5H_2O$ **(2)**	37,735	$\pi \rightarrow \pi^*$	9302	829	0.80	3.03
	25,640	$^3A_{1g} \rightarrow {}^3T_{1g}$ (P)				
	14,815	$^3A_{1g} \rightarrow {}^3T_{1g}$				
	13,900	$^3A_{1g} \rightarrow {}^1E_g$				
	9260	$^3A_{1g} \rightarrow {}^3T_{2g}$				
$[Ni(5\text{-}MeBzIm)_2(acr)_2(H_2O)]$ **(3)**	36,360	$\pi \rightarrow \pi^*$	9216	899	0.87	3.04
	25,315	$^3A_{1g} \rightarrow {}^3T_{1g}$ (P)				
	14,815	$^3A_{1g} \rightarrow {}^3T_{1g}$				
	13,500	$^3A_{1g} \rightarrow {}^1E_g$				
	9220	$^3A_{1g} \rightarrow {}^3T_{2g}$				
$[Ni(5,6\text{-}Me_2BzIm)_2(acr)_2]$ **(4)**	38,460	$\pi \rightarrow \pi^*$	9302	903	0.88	2.82
	36,360					
	25,975	$^3A_{1g} \rightarrow {}^3T_{1g}$ (P)				
	15,500	$^3A_{1g} \rightarrow {}^3T_{1g}$				
	13,515	$^3A_{1g} \rightarrow {}^1E_g$				
	9300	$^3A_{1g} \rightarrow {}^3T_{2g}$				

These data are in good agreement with the results obtained by elemental and thermal analysis, confirming the proposed formulation of complexes.

Proposed coordination for nickel(II) complexes (1)–(4)

Evaluating the results obtained from experimental data, the most probable coordination for complexes (**1**)–(**4**) is that presented in Fig. 2. All complexes present an octahedral arrangement around nickel ion. For all nickel complexes, the blue color was ascribed to $[NiN_2O_4]$ chromophore.

In the case of complex (**1**), two benzimidazoles that act as monodentate are *cis*-positioned, one acrylate is unidentate and the other one is bidentate chelate. One water molecule completes the coordination sphere.

For complexes (**2**) and (**3**), the coordination sphere is made up of 2-methylbenzimidazole/5-methylbenzimidazole *trans*-positioned units, one acrylate that acts unidentate, other one bidentate chelate, and one water molecule.

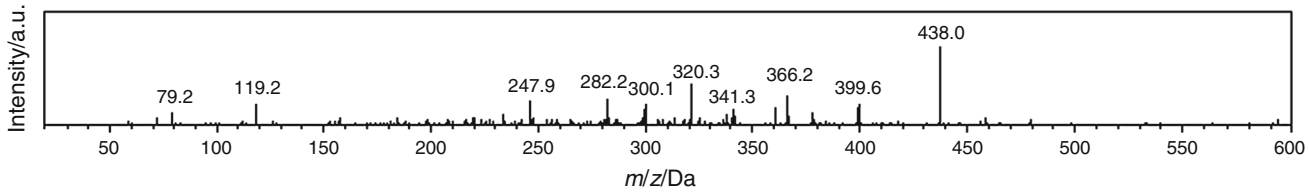

Fig. 1 ESI–MS spectrum of complex $[Ni(HBzIm)_2(acr)_2(H_2O)]\cdot 3H_2O$ (**1**)

Fig. 2 Proposed coordination for nickel(II) complexes (**1**)–(**4**)

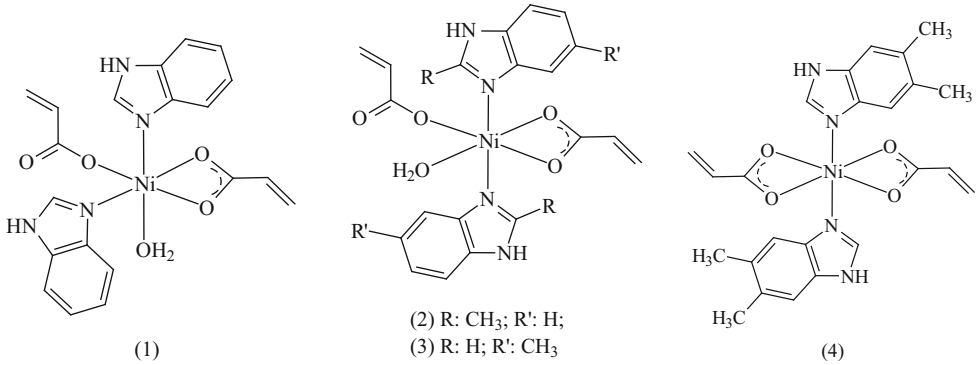

Complex (**4**) is anhydrous and contains two 5,6-dimethylbenzimidazole molecules *trans*-positioned and two acrylates coordinated in a bidentate chelate fashion.

Thermal analysis

Thermal analysis was used in order to characterize the thermal stability and to confirm the chemical formulas of compounds (**1**)–(**4**). Table 4 contains information regarding the thermal parameters and the temperature decomposition ranges.

*Complex $[Ni(HBzIm)_2(acr)_2(H_2O)]\cdot 3H_2O$ (**1**)*

Thermal decomposition of complex (**1**) occurs in several well-defined steps as it can be observed in Fig. 3. First step starts at 153 °C, and it corresponds to water molecules loss (calc. mass loss 14.2 %, exp. 14.1 %), this step being accompanied by an endothermic effect. The anhydrous compound resulted in this first step is thermally stable in a temperature range of 45 °C. The next two steps are starting above 260 °C, with the oxidative degradation of one benzimidazole molecule (calc. mass loss 23.2 %, exp. 23.1 %), and above 350 °C the second benzimidazole molecule is lost (calc. mass loss 23.2 %. exp. 23.4 %), both decomposition steps being accompanied by exothermic effects, as it can be observed from the DTA curve (Fig. 3). The last step of thermal decomposition corresponds to nickel acrylate conversion to nickel oxide (calc. mass loss 24.8 %, exp. 24.5 %), which was confirmed by powder XRD analysis of the final residue, cf JCPDS Card No. 47-1049 (see supplementary material, Fig. 3S).

*Complex $[Ni(2\text{-}MeBzIm)_2(acr)_2(H_2O)]\cdot 1.5H_2O$ (**2**)*

It can ascertain six well-defined decomposition steps in the thermal behavior of complex (**2**) (Fig. 4). The first two steps, in the 90–260 °C temperature range, correspond to water molecules loss. First are released the uncoordinated water molecules (calc. mass loss 5.3 %, exp. 5.4 %) [30, 31]. The compound resulted in the first step $[Ni(2\text{-}MeBzIm)_2(acr)_2(H_2O)]$ is stable on a 30 °C temperature range. The second decomposition step is assigned to the final dehydration process (calc. mass loss 3.5 %, exp. 3.6 %), and the anhydrous compound resulted in this step is stable on a 20 °C temperature range. Above 280 °C, one molecule of 2-methylbenzimidazole is released in an oxidative degradation process accompanied by an exothermic effect (calc. mass loss 25.9 %, exp. 25.8 %); in the temperature range 380–545 °C, the second 2-methylbenzimidazole is released (calc. mass loss 25.9 %, exp. 25.7 %), process accompanied also by an exothermic effect. Above 545 °C, the conversion of nickel acrylate to nickel carbonate occurs (calc. mass loss 16.1 %, exp. 16.3 %). Starting with 700 °C, one can observe the last thermal decomposition step being represented by decomposition of nickel carbonate to nickel oxide (calc. mass loss 8.6 %, exp. 8.4 %), and the final residue (calc. mass 14.7 %, exp. 14.8 %) was confirmed by powder X-ray diffraction analysis.

Table 4 Thermal decomposition data (in air flow) for nickel complexes (**1**)–(**4**)

Complex	Step	Thermal effect	Temperature range/°C	Δm_{exp}/%	Δm_{calc}/%	Evolved moieties
$[Ni(HBzIm)_2(acr)_2(H_2O)]\cdot 3H_2O$ **(1)**	1	Endothermic	153–215	14.1	14.2	$-4(H_2O)$
	2	Exothermic	260–350	23.1	23.2	–(HBzIm)
	3	Exothermic	350–470	23.4	23.2	–(HBzIm)
	4	Exothermic	470–630	24.5	24.8	$-(C_6H_6O_3)$
	Residue (NiO)			14.9	14.7	
$Ni(2\text{-}MeBzIm)_2(acr)_2(H_2O)]\cdot 1.5H_2O$ **(2)**	1	Endothermic	90–150	5.4	5.3	$-1.5(H_2O)$
	2	Endothermic	180–260	3.6	3.5	$-(H_2O)$
	3	Exothermic	280–380	25.8	25.9	–(2-MeBzIm)
	4	Exothermic	380–545	25.7	25.9	–(2-MeBzIm)
	5	Exothermic	545–700	16.3	16.1	$-(C_5H_6O)$
	6	Exothermic	700–880	8.4	8.6	$-(CO_2)$
	Residue (NiO)			14.8	14.7	
$[Ni(5\text{-}MeBzIm)_2(acr)_2(H_2O)]$ **(3)**	1	Endothermic	155–190	3.6	3.7	$-(H_2O)$
	2	Exothermic	290–775	80.7	80.8	–2(5-MeBzIm); $-(C_5H_6O)$; $-(CO_2)$
	Residue (NiO)			15.7	15.5	
$[Ni(5,6\text{-}Me_2BzIm)_2(acr)_2]$ **(4)**	1	Exothermic	250–410	29.1	29.6	$-(5,6Me_2BzIm)$;
	2	Exothermic	410–710	46.6	46.3	$-(5,6Me_2BzIm)$ $-(C_5H_6O)$;
	3	Exothermic	710–870	9.1	8.9	$-(CO_2)$
	Residue (NiO)			15.2	15.1	

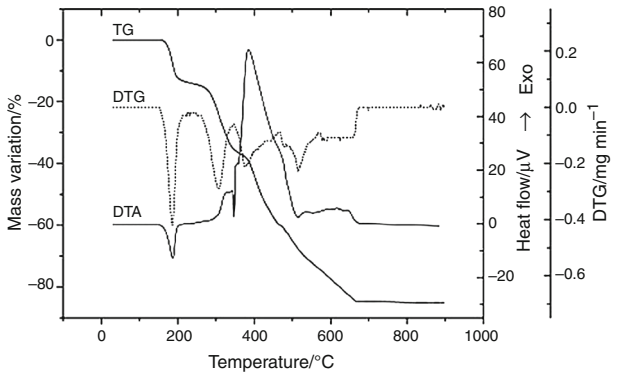

Fig. 3 Thermoanalytical (TG, DTG and DTA) curves of $[Ni(HBzIm)_2(acr)_2(H_2O)]\cdot 3H_2O$ (**1**) in air flow at 10 K min^{-1}

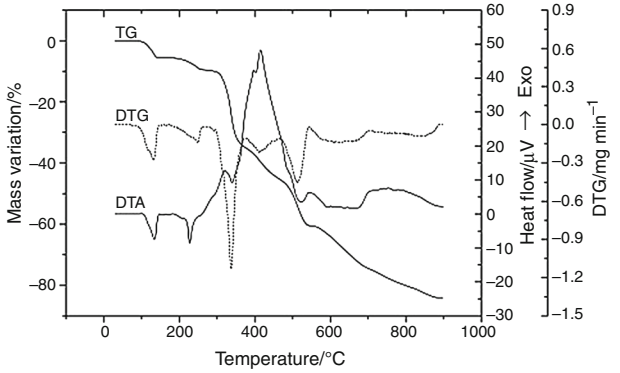

Fig. 4 Thermoanalytical (TG, DTG and DTA) curves of $[Ni(2\text{-}MeBzIm)_2(acr)_2(H_2O)]\cdot 1.5H_2O$ (**2**) in air flow at 10 K min^{-1}

Complex $[Ni(5\text{-}MeBzIm)_2(acr)_2(H_2O)]$ (3)

As it can be seen in Fig. 5, the thermal decomposition of $[Ni(5\text{-}MeBzIm)_2(acr)_2(H_2O)]$ (**3**) occurs in two steps. The thermal decomposition is starting at 155 °C with the release of one water molecule (calc. mass loss 3.7 %, exp. 3.6 %), accompanied by an endothermic effect. The anhydrous compound is stable in a temperature range of 100 °C. In the range of 290–775 °C, several overlapped exothermic processes like oxidative degradation of 5-methylbenzimidazole, acrylate conversion to carbonate and the decomposition of nickel carbonate are observed. The final product of the thermal decomposition above 775 °C is nickel oxide (calc. mass 15.5 %, exp. 15.7 %), which was confirmed by powder XRD analysis.

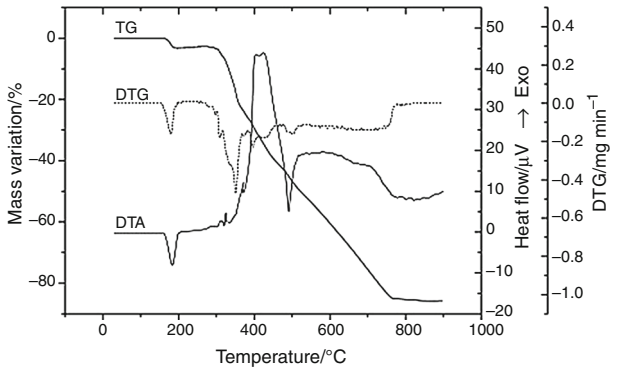

Fig. 5 Thermoanalytical (TG, DTG and DTA) curves of [Ni(5-MeBzIm)$_2$(acr)$_2$(H$_2$O)] (**3**) in air flow at 10 K min^{-1}

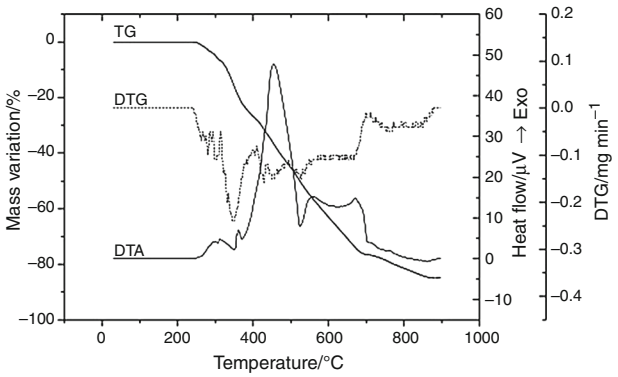

Fig. 6 Thermoanalytical (TG, DTG and DTA) curves of [Ni(5,6-Me$_2$BzIm)$_2$(acr)$_2$] (**4**) in air flow at 10 K min^{-1}

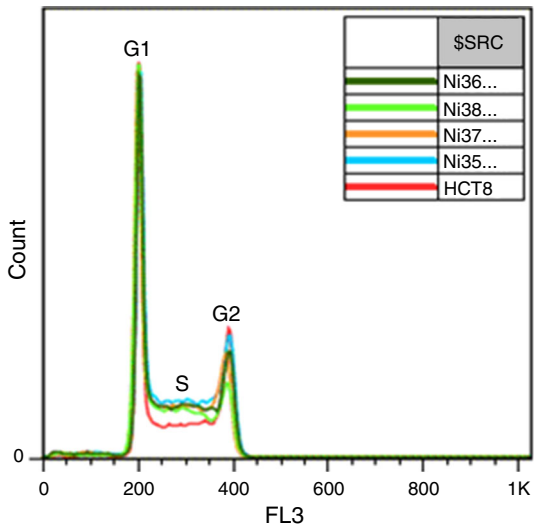

Fig. 7 Flow cytometry overlapped histogram and percentages of HCT-8 cells found in the different cell cycle phases, after treatment with nickel (II) complexes

Table 5 Complexes effect upon the HCT-8 cell cycle progression

	Freq. G1	Freq. S	Freq. G2
HCT-8	34.12	45.22	17.48
Ni35 (**1**)	29.35	53.08	12.96
Ni36 (**2**)	30.27	53.15	11.93
Ni37 (**3**)	30.37	52.59	11.27
Ni38 (**4**)	30.04	53.21	12.12

*Complex [Ni(5,6-Me$_2$BzIm)$_2$(acr)$_2$] (**4**)*

This compound is thermally stable up to 250 °C (as depicted in Fig. 6); first decomposition step consists in oxidative degradation of one 5,6-dimethylbenzimidazole molecule (calc. mass loss 29.6 %, exp. 29.1 %), process accompanied by an exothermic effect. The next step of thermal decomposition is a sum of several processes like the oxidative degradation of the other 5,6-dimethylbenzimidazole molecule and the conversion of nickel acrylate into nickel carbonate (calc. mass loss 46.3 %, exp. 46.6 %), all these processes producing a strong exothermic effect. Finally, nickel carbonate decomposes to nickel oxide (calc. mass 15.1 %, exp. 15.2 %) whose formation is confirmed by powder XRD analysis.

Microbiological assay

The antimicrobial activity for nickel(II) complexes was qualitatively evaluated against several microbial strains, and it was compared with DMSO activity which was the solvent used to dissolve all the complexes. All complexes presented superior diameters of the inhibition zones compared with DMSO, against all tested microbial strains. The next goal was to determine quantitatively the antimicrobial activity by assessing the minimum inhibitory concentration value MIC (μg mL^{-1}).

The biological investigations allowed to conclude:

- Complexes (**1**)–(**4**) exhibited moderated antimicrobial activity with MIC values of 500 μg mL^{-1} against *Enterococcus faecium* E5, *Escherichia coli* ATCC 25922 and *Candida albicans* 1760;
- Complexes (**1**), (**3**) and (**4**) presented an inhibitory effect of the microbial adherence on inert substrate against *Enterococcus faecium* E5, and complex (**2**) against *Klebsiella pneumoniae* with a biofilm minimum inhibitory concentration BMIC of 250 μg mL^{-1}.

Literature data reveals low to moderate antimicrobial activity of similar octahedral Ni(II) complexes [32, 44–47]. This behavior is due to nickel (II) strong preference for the octahedral stereochemistry that limits the interaction with bacterial or fungal strains.

Cytotoxicity

All tested complexes slightly decreased the number of cells found in G1 and G2 phases and increased the percentage of cells found in the S phase. However, the tested complexes proved to be no cytotoxic, as no apoptosis peak was recorded on the flow cytometry histograms obtained for the HCT-8 cells treated with the respective complexes (Fig. 7; Table 5).

Conclusions

Four new and nickel (II) complexes with acrylate and benzimidazole/benzimidazole derivatives were synthesized, structurally and biologically characterized. Thermal analysis indicated a great thermal stability for these nickel compounds. Thermal decomposition trend is maintained for this class of complexes, several steps being observed like water molecules loss, benzimidazole oxidative degradation, nickel acrylate conversion into nickel carbonate and as a final step the nickel carbonate decomposition to nickel oxide, which was the final residue for all four complexes. The biological studies revealed that these new nickel complexes (**1**)–(**4**) present moderate antimicrobial activity, and this fact can be ascribed to the coordinative saturation of the nickel (II) complexes, the octahedral arrangement around nickel ion limiting the interaction with bacterial or fungal strains. The complexes are non-toxic as cytotoxicity studies proved.

Acknowledgements I. D. Vlaicu acknowledges the financial support to the Sectorial Operational Programme Human Resources Development (SOP HRD), financed from the European Social Fund and by the Romanian Government under the contract number SOP HRD/107/1.5/S/82514. This work was partially supported by University of Bucharest.

References

1. Aijaz A, Lama P, Sañudo EC, Mishra R, Bharadwaj PK. Coordination polymers of various architectures built with mixed imidazole/benzimidazole and carboxylate donor ligands and different metal ions: syntheses, structural features and magnetic properties. New J Chem. 2010;34:2502–14.
2. Velík J, Baliharová V, Fink-Gremmels J, Bull S, Lamka J, Skálová L. Benzimidazole drugs and modulation of biotransformation enzymes. Res Vet Sci. 2004;76(2):95–108.
3. Al-Khodir FAI, Refat MS. Synthesis, spectroscopic, thermal analyses, and anti-cancer studies of metalloantibiotic complexes of Ca(II), Zn(II), Pt(II), Pd(II), and Au(III) with albendazole drug. Russ J Gen Chem. 2015;85(7):1734–44.
4. Shaker SA, Khaledi H, Cheah S-C, Ali HM. New Mn(II), Ni(II), Cd(II), Pb(II) complexes with 2-methylbenzimidazole and other ligands. Synthesis, spectroscopic characterization, crystal structure, magnetic susceptibility and biological activity studies. Arab J Chem. 2012;. doi:10.1016/j.arabjc.2012.06.013.
5. Podunavac-Kuzmanović SO, Cvetković DM. Antibacterial evaluation of some benzimidazole derivatives and their zinc (II) complexes. J Serb Chem Soc. 2007;72(5):459–66.
6. Devereux M, O'Shea D, O'Connor M, Grehan H, Connor G, McCann M, Rosair G, Lyng F, Kellett A, Walsh M, Egan D, Thati B. Synthesis, catalase, superoxide dismutase and antitumour activities of copper(II) carboxylate complexes incorporating benzimidazole, 1,10-phenanthroline and bipyridine ligands: X-ray crystal structures of $[Cu(BZA)_2(bipy)(H_2O)]$, $[Cu(SalH)_2(BZDH)_2]$ and $[Cu(CH_3COO)_2(5,6\text{-}DMBZDH)_2]$ ($SalH_2$ = salicylic acid; BZAH = benzoic acid; BZDH = benzimidazole and 5,6-DMBZDH = 5,6-dimethylbenzimidazole). Polyhedron. 2007;26(15):4073–84.
7. Wang Z-W, Yu M, Li T, Meng X-R. Syntheses, crystal structures and fluorescent properties of 2-D Cd(II) complexes based on 2-(1H-imidazol-1-methyl)-1H-benzimidazole and 1,2,4,5-benzenetetracarboxylate ligands. J Coord Chem. 2013;66(23):4163–77.
8. Yang R, Ge M, Van Hecke K, Cui G-H. Synthesis, crystal structure and catalytic properties of a new 2D nickel (II) bis(benzimidazole). Chin J Struct Chem. 2014;33(12):1819–25.
9. Shi Q, Chen L, Liu D, Wu J, Wu L, Zhu L, Cheng Q, Lu R, Fan D, Lü X. A new tetranuclear nickel complex based on the benzimidazole ligand for the controllable polymerization of methyl methacrylate. Inorg Chem Commun. 2013;29:22–6.
10. Pandey VK, Upadhyay M, Upadhyay M, Gupta VD, Tandon M. Benzimidazolyl quinolinyl mercaptotriazoles as potential antimicrobial and antiviral agents. Acta Pharm. 2005;55:47–56.
11. Podunavac-Kuzmanović SO, Leovac VM, Cvetković DM. Antibacterial activity of cobalt (II) complexes with benzimidazole derivatives. J Serb Chem Soc. 2008;73(12):1153–60.
12. Brahmachari G. Green synthetic approaches for biologically relevant heterocycles: an overview. New Bengal: Elsevier; 2014.
13. Barker HA, Smyth RD, Weissbach H, Toohey JI, Ladd JN, Volcani BE. Isolation and properties of crystalline cobamide coenzymes containing benzimidazole or 5,6-dimethylbenzimidazole. J Biol Chem. 1960;235(2):480–8.
14. Lin D-D, Liu Y, Xu D-J. Tetrakis(benzimidazole-kN)(malonato-k2O, O')cobalt(II). Acta Cryst. 2003;E59:m771–3.
15. Xue Y-H, Lin D-D, Xu D-J. Polymeric aqua(benzimidazole-kN)(μ-malonato)cobalt(II). Acta Cryst. 2003;E59:m750–2.
16. Liu Y, Xu D-J, Lin D-D, Yin K-L. Catena-Poly[[diaquabis(benzimidazole-kN)cobalt(II)]-μ-fumarato-$k^2O^1:O^4$]. Acta Cryst. 2003;E59:m753–5.
17. Song W-D, Wang H, Qin P-W, Li S-J, Hu S-W. Pentaaqua (1H-benzimidazole-5,6-dicarboxylato-kN^3)nickel (II) pentahydrate. Acta Cryst. 2009;E65:m672.
18. Xie Y, Xing Y-H, Wang Z, Zhao H-Y, Zeng X-Q, Ge M-F, Niu S-Y. Synthesis, structures and luminescent properties of novel coordination polymers constructed by lanthanide salts and benzimidazole-5,6-dicarboxylic acid. Inorg Chim Acta. 2010;363:918–24.
19. Liu Z, Chen Y, Liu P, Wang J, Huang M. Cadmium(II) and cobalt(II) complexes generated from benzimidazole-5-carboxylate: self-assembly by hydrogen bonding and interactions. J Solid State Chem. 2005;178(7):2306–12.
20. Fan J, Cai S-L, Zheng S-R, Zhang W-G. Two mononuclear octahedral complexes with benzimidazole-2-carboxylate: supramolecular networks constructed by hydrogen bonds. Acta Cryst. 2011;C67:m346–50.
21. Badea M, Olar R, Marinescu D, Vasile G. Thermal behavior of new triazole derivative complexes. J Therm Anal Calorim. 2008;92:209–14.
22. Badea M, Olar R, Marinescu D, Lazăr V, Chifiriuc C, Vasile G. Thermal behaviour of new biological active cadmium mixed ligands complexes. J Therm Anal Calorim. 2009;97:781–5.

23. Vlaicu ID, Constand M, Olar R, Marinescu D, Grecu MN, Lazar V, Chifiriuc MC, Badea M. Thermal stability of new biologic active copper (II) complexes with 5,6-dimethylbenzimidazole. J Therm Anal Calorim. 2013;113:1369–77.
24. Badea M, Vlaicu ID, Olar R, Constand M, Bleotu C, Chifiriuc MC, Marutescu L, Lazar V, Grecu MN, Marinescu D. Thermal behaviour and characterization of new biologically active Cu(II) complexes with benzimidazole as main ligand. J Therm Anal Calorim. 2014;118:1119–33.
25. Matei L, Bleotu C, Baciu I, Draghici C, Ionita P, Paun A, Chifiriuc MC, Sbarcea A, Zarafu I. Synthesis and bioevaluation of some new isoniazid derivatives. Bioorg Med Chem. 2013;21(17):5355–61.
26. Singh N, Pandurangan A, Rana K, Anand P, Ahamad A, Tiwari AK. Benzimidazole: a short review of their antimicrobial activities. Int Curr Pharm J. 2012;1(5):119–27.
27. Arali VH, Revankar VK, Mahale VB, Kulkarni PJ. Cobalt(II), nickel(II) and copper(II) with 2-substituted benzimidazole complexes. Transit Met Chem. 1994;19:57–60.
28. El-Sherif AA. Synthesis, solution equilibria and antibacterial activity of Co(II) with 2-(aminomethyl)-benzimidazole and dicarboxylic acids. J Solut Chem. 2010;39:1562–81.
29. Murthy YLN, Durga G, Jha A. Synthesis, characterization, and antimicrobial activity of some new 2-diazo-benzimidazole derivatives and their Ni(II), Cu(II), and Ag(I) complexes. Med Chem Res. 2013;22:2266–72.
30. Abdel-Ghani NT, El-Ghar MFA, Mansour AM. Novel Ni(II) and Zn(II) complexes coordinated by 2-arylaminomethyl-1H-benzimidazole: molecular structures, spectral, DFT studies and evaluation of biological activity. Spectrochim Acta A Mol Biomol Spectrosc. 2013;104:134–42.
31. Mansour AM, El Bakry EM, Abdel-Ghani NT. Co(II), Ni(II) and Cu(II) complexes of methyl-5-(Phenylthio)benzimidazole-2-carbamate: molecular structures, spectral and DFT calculations. J Mol Struct. 2016;1111:100–7.
32. El-wakiel N, El-keiy M, Gaber M. Synthesis, spectral, antitumor, antioxidant and antimicrobial studies on Cu(II), Ni(II) and Co(II) complexes of 4-[(1H-Benzoimidazol-2-ylimino)-methyl]-benzene-1,3-diol. Spectrochim Acta A Mol Biomol Spectrosc. 2015;147:117–23.
33. Nakamoto K. Infrared and Raman spectra of inorganic and coordination compounds. New York: Wiley; 1986.
34. Oldham C. Carboxylates, squarates and related species. In: Wilkinson G, Gillard RD, McCleverty JA, editors. Comprehensive coordination chemistry. Oxford: Pergamon Press; 1987.
35. Deacon GB, Philips RJ. Relationships between the carbon-oxygen stretching frequencies of carboxylato complexes and the type of carboxylate coordination. Coord Chem Rev. 1980;33:227–50.
36. Matelková K, Boča R, Dlháň L, Herchel R, Moncol J, Svoboda I, Mašlejová A. Dinuclear and polymeric (l-formato)nickel(II) complexes: synthesis, structure, spectral and magnetic properties. Polyhedron. 2015;95:45–53.
37. Xue Y-H, Liu J-G, Xu D-J. A helical polymeric complex, tris(benzimidazole)nickel(II) (μ-maleato). J Coord Chem. 2005; 58(12):1071–6.
38. Lever ABP. Inorganic electronic spectroscopy. Amsterdam: Elsevier; 1986.
39. Hathaway BJ, Billing DE. The electronic properties and stereochemistry of mono-nuclear complexes of the copper(II) ion. Coord Chem Rev. 1970;5:143–207.
40. Brezeanu M, Patron L, Andruh M. Polynuclear complexes and their applications. Bucharest: Romanian Academy Ed.; 1986.
41. Gispert JR. Coordination chemistry. Weinheim: Wiley; 2008.
42. König E. The nephelauxetic effect. Calculation and accuracy of the interelectronic repulsion parameters I. Cubic high-spin d^2, d^3, d^7 and d^8 systems. Struct Bond. 1972;9:175–372.
43. Ferguson J. Spectroscopy of 3d complexes. Progress in inorganic chemistry. New York: Lt J Lippard Ed, Interscience Publishers; 1970.
44. Podunavac-Kuzmanovic S, Leovac VM, Cetkovic G, Markov S. Synthesis, physico-chemical characterization and biological activity of copper(II) and nickel(II) complexes with 1-benzoyl-2-methylbenzimidazole derivatives. Acta Period Technol. 2002;33:151–7.
45. Vlaicu ID, Mirica G, Bucur M, Marutescu L, Chifiriuc C, Olar R, Badea M. Synthesis, physico-chemical characterization and biologic activity of a new nickel complex with 2-cyanoguanidine. Ann Univ Bucur Chim. 2010;19(1):19–22.
46. Olar R, Vasile Scaeteanu G, Vlaicu ID, Marutescu L, Badea M. Synthesis, physico-chemical characterization and thermal behavior of new complexes with N_4O_2 donor set. J Therm Anal Calorim. 2014;118:1195–202.
47. Kopel P, Wawrzak D, Langer V, Cihalova K, Chudobova D, Vesely R, Adam V, Kizek R. Biological activity and molecular structures of bis(benzimidazole) and trithiocyanurate complexes. Molecules. 2015;20:10360–76.